



# Magneto-optical properties of one-dimensional aperiodic magneto-phonic crystals based on Kolakoski sequences

Tahereh Sadat Parvini<sup>1</sup> · Mehdi Khazaei Nezhad<sup>2</sup>

Received: 24 May 2022 / Accepted: 28 September 2022 / Published online: 8 October 2022  
© The Author(s) 2022

## Abstract

Magneto-optical properties of one-dimensional aperiodic structures formed by stacking together magnetic and nonmagnetic layers according to the Kolakoski self-generation scheme are studied theoretically using the  $4 \times 4$  transfer matrix method. The effect of the generation stage of the sequence, and the helicity and direction of light propagation through the magneto-phonic crystals on the transmission/reflection spectra as well as Faraday and ellipticity rotations, have been investigated. Our results reveal that this kind of aperiodic magneto-phonic crystals can be used for the fabrication of multifrequency laser cavities, and optical filters/sensors.

## 1 Introduction

Nowadays, the advances in deposition and crystal growth technologies have caused the periodic, quasiperiodic, aperiodic, and random photonic crystals (PhCs) to attract extensive interest and emerged as a new potential platform for the development of high harmonic generators [1–5], terahertz emitters [6, 7], optical sensors/filters [8–11] and so on. PhCs with magnetic and nonmagnetic constituents are known as magneto-phonic crystal (MPCs). Physically, destructive interference of scattered waves at the boundary of different layers in PhCs leads to the formation of band gaps that prevent waves with certain frequencies from traveling through the structure. The presence of the nonreciprocal and unidirectional photonic bandgap (PBG) is the most prominent property of MPCs which can be tuned by an external magnetic field [12–16]. The enhancement of magneto-optical effects, such as transmittance and a Faraday rotation, are other important features of MPCs. This enhancement can be attributable to the constructive interferences of light within magnetic layers that cause the light localization and

light-matter interaction enhancement. Translational-symmetry breaking in MPCs with quasi-periodic, aperiodic, and random arrangement cause light localization enhancement as well as the emergence of defect mode(s) [17–20]. Random MPCs are built without specific rules, while quasi-periodic and aperiodic ones are fabricated according to certain substitutional rules and have an intrinsic symmetry of self-similarity, which manifests itself in the structure of their Fourier spectra [21]. However, the Fourier spectra of quasi-periodic structures like Fibonacci consist of isolated Bragg peaks with incommensurate periods, while aperiodic structures such as Thue–Morse and Rudin–Shapiro possess fractal and flat Fourier spectra with a variety of unique technological applications [22]. It has been proven that these structures combine strong magneto-optical effects with PBG properties effectively [23–27].

The Kolakoski self-generating sequence is another kind of aperiodic structure that has attracted significant interest in different branches of science, including fabricating aperiodic MPCs with applications in linear/nonlinear optical devices [28–30]. In this work, we study the magneto-optical properties of one-dimensional aperiodic MPCs formed by stacking magnetic and nonmagnetic materials according to the Kolakoski generation scheme. By using the  $4 \times 4$  transfer matrix method (TMM), the transmittance, reflectance, Faraday rotation, and ellipticity are investigated as a function of the frequency, polarization, and angle of incident light for different numbers of layers  $\mathcal{N}$ .

✉ Tahereh Sadat Parvini  
tahereh.parvini@uni-greifswald.de  
Mehdi Khazaei Nezhad  
khazaeinezhad@um.ac.ir

<sup>1</sup> Institut für Physik, Universität Greifswald, Greifswald, Germany

<sup>2</sup> Department of Physics, Faculty of Science, Ferdowsi University of Mashhad, Mashhad, Iran

## 2 Theory

### I. 4×4 Transmission matrix formalism

One of the possible configurations of the structure under consideration with  $\mathcal{N}=14$  layers is schematically depicted in Fig. 1. It is assumed that the letters M denote the magnetic layer of thickness  $d_M$  and N is the nonmagnetic layer of thickness  $d_N$ . The plane electromagnetic wave of frequency  $\omega$  propagates in the  $yz$  plane with the wavevector  $\mathbf{k} = \{0, k_y, k_z\}$ .

At optical frequencies, propagation of electromagnetic waves in a material is determined by the properties of the dielectric permittivity tensors  $\hat{\epsilon}$  and  $\hat{\mu}$ . In a medium uniformly magnetized along the  $z$ -axis (polar geometry), the tensors have the following form [31–33]:

$$\hat{\epsilon} = \begin{pmatrix} \epsilon_{xx} & \epsilon_{xy} & 0 \\ -\epsilon_{xy} & \epsilon_{xx} & 0 \\ 0 & 0 & \epsilon_{zz} \end{pmatrix} \quad \hat{\mu} = \begin{pmatrix} \mu_{xx} & \mu_{xy} & 0 \\ -\mu_{xy} & \mu_{xx} & 0 \\ 0 & 0 & \mu_{zz} \end{pmatrix}. \quad (1)$$

Within the optical wavelength region,  $\hat{\mu}$  differs only slightly from unity ( $\hat{\mu} = \mu\delta_{ij}$ , where  $\delta_{ij}$  is Kronecker delta symbol). Furthermore, the non-magnetic crystal with a cubic symmetry is characterized by the diagonal tensors  $\hat{\epsilon}_N = \epsilon\delta_{ij}$ .

In the following, to study the magneto-optical properties of one-dimensional aperiodic MPCs, we use the 4×4 transfer matrix method [34–36] which couples the field amplitudes at the structure input and output. According to this formalism, the transfer matrix  $\hat{T}$  has the following form:

$$\hat{T} = \hat{A}_{bg}^{-1} \prod_{i=N}^1 \hat{A}_i \hat{E}_i \hat{A}_i^{-1} \hat{A}_{bg}, \quad (2)$$

where  $\hat{E}_i$  is the propagation matrix of the four eigenmodes inside the layer  $i$ ,

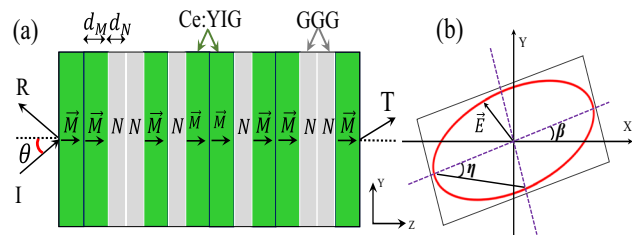


**Fig. 1** **a** Polar geometry of an aperiodic stack composed of magnetized ferrite and isotropic dielectric layers with Kolakoski arrangement at the eighth generation stage ( $\mathcal{N}=14$ ). **b** The polarization ellipse of the outgoing beams under normal electromagnetic wave incidence, with Faraday and ellipticity angles  $\beta$  and  $\eta$ , respectively

$$\hat{E}_i = \begin{pmatrix} e^{ik_z^{(1)}z} & 0 & 0 & 0 \\ 0 & e^{ik_z^{(2)}z} & 0 & 0 \\ 0 & 0 & e^{ik_z^{(3)}z} & 0 \\ 0 & 0 & 0 & e^{ik_z^{(4)}z} \end{pmatrix}, \quad (3)$$

with wavevectors  $k_z^{(j)}$ , ( $j = 1...4$  of the normal modes). Depending on the characteristics of each layer in MPC, the electromagnetic field of light that travels inside that is split into different modes with different  $k_z$ s [32]. Matrix  $\hat{A}_i$  relates the total electric  $E_{xy}$  and magnetic  $H_{xy}$  fields of the plane electromagnetic waves at the boundary of the layer to the amplitudes of the eigenmodes.  $\hat{A}_{bg}$  is related to the surrounding medium, with  $i=YIG$  or  $GGG$ . By solving the Maxwell equations we can find the elements of the matrices  $\hat{A}_i$ . In this case, the electromagnetic wave splits into four modes with wavevectors  $k_z^{(1)} = k_+$ ,  $k_z^{(2)} = -k_+$ ,  $k_z^{(3)} = k_-$ , and  $k_z^{(4)} = -k_-$  where:

$$k_{\pm} = \sqrt{\epsilon_{xx}\Omega^2 - k_y^2 \pm \sqrt{D_p}}, \quad (4)$$

$D_p = -\epsilon_{xy}^2\Omega^4 + \frac{\epsilon_{xy}^2}{\epsilon_{zz}}\Omega^2k_y^2$ , and normalized frequency is  $\Omega = \omega/c$ . The explicit form of the matrix  $\hat{A}$  for the polar magnetic layer can be written as

$$\hat{A}_{YIG} = \begin{pmatrix} V^+ & -V^+ & F^- & F^- \\ G^+ & -G^+ & 1 & 1 \\ F^+ & F^+ & -V^- & V^- \\ 1 & 1 & -G^- & G^- \end{pmatrix}, \quad (5)$$

$V^{\pm} = \frac{v^{\pm}}{z^{\pm}}$ ,  $G^{\pm} = \frac{g^{\pm}}{z^{\pm}}$ , and  $F^{\pm} = \frac{f^{\pm}}{z^{\pm}}$ , where

$$\begin{aligned} z^+ &= \epsilon_{xx}[\epsilon_{xx}\Omega^2 - k_y^2 - k_+^2]k_+, \\ v^+ &= \epsilon_{xx}[\epsilon_{xx}\Omega^2 - k_y^2 - k_+^2]\Omega, \\ g^+ &= i\epsilon_{xy}[\epsilon_{xx}\Omega^2 - k_y^2]\Omega, \\ f^+ &= -i\epsilon_{xx}\epsilon_{xy}\Omega^2k_+. \end{aligned} \quad (6)$$

The values  $z^-$ ,  $v^-$ ,  $g^-$  and  $f^-$  can be obtained from  $z^+$ ,  $v^+$ ,  $g^+$  and  $f^+$  respectively, by the replacement ( $\epsilon, k_+ \leftrightarrow \mu, k_-$ ) [32]. For the normal incidence, wavevectors becomes  $k_{\pm} = \sqrt{\epsilon_{xx} \pm i\epsilon_{xy}}\Omega$ , and the matrix  $\hat{A}$  reduces to the form

$$\hat{A}_{YIG} = \begin{pmatrix} P_+ & -P_+ & -i & -i \\ -iP_+ & iP_+ & 1 & 1 \\ i & i & -1/P^- & 1/P^- \\ 1 & 1 & -i/P^- & i/P^- \end{pmatrix}, \quad (7)$$

where  $P_+ \equiv \sqrt{\frac{\mu_{xx} + i\mu_{xy}}{\epsilon_{xx} + i\epsilon_{xy}}}$  and  $P_- \equiv \sqrt{\frac{\epsilon_{xx} - i\epsilon_{xy}}{\mu_{xx} - i\mu_{xy}}}$ .

Beside, the wavevectors in the nonmagnetic cubic medium are

$$k_{\pm}^2 = n^2\Omega^2 - k_y^2, \tag{8}$$

with  $n = \sqrt{\epsilon}$  and the  $\hat{A}$ -matrix of the layer is

$$\hat{A}_{GGG} = \begin{pmatrix} \Omega/k_z & -\Omega/k_z & 0 & 0 \\ 0 & 0 & 1 & 1 \\ 0 & 0 & -\epsilon\Omega/k_z & \epsilon\Omega/k_z \\ 1 & 1 & 0 & 0 \end{pmatrix}. \tag{9}$$

In the case of normal incidence  $k_{\pm} = \pm n\Omega$ , and

$$\hat{A}_{GGG} = \begin{pmatrix} \frac{1}{n} & \frac{-1}{n} & 0 & 0 \\ 0 & 0 & 1 & 1 \\ 0 & 0 & \frac{-\epsilon}{n} & \frac{\epsilon}{n} \\ 1 & 1 & 0 & 0 \end{pmatrix}. \tag{10}$$

Following the theory provided in [32], we can write the transmitted  $t^s, t^p$  and reflected  $r^s, r^p$  light magnitudes in terms of the incident light magnitudes  $a^s, a^p$  using the transmission matrix in Eq. 2 as follows

$$\begin{bmatrix} t^s \\ 0 \\ t^p \\ 0 \end{bmatrix} = \hat{S}_f \hat{T} \hat{S}_i^{-1} \begin{bmatrix} a^s \\ r^s \\ a^p \\ r^p \end{bmatrix}, \tag{11}$$

where subscripts p and s correspond to the p-polarized and s-polarized electromagnetic waves, respectively. With the assumption that the 1D MPC is embedded in the isotropic dielectric media  $i$  before and  $f$  behind that with refractive index  $n_i$  and  $n_f$  respectively, the  $S$  matrices read

$$\hat{S}_{i,f} \equiv \frac{1}{\cos\theta_{i,f}} \begin{bmatrix} n_{i,f}^{-1} & 0 & 0 & 0 \\ 0 & n_{i,f}^{-1} & 0 & 0 \\ 0 & 0 & 1 & 0 \\ 0 & 0 & 0 & 1 \end{bmatrix}, \tag{12}$$

where  $\theta_{i,f}$  is the angle between the wavevector and  $z$ -axis in media  $i$  and  $f$ . Accordingly, intensities of the transmitted and reflected light are given by  $T = |t^p|^2 + |t^s|^2$  and  $R = |r^p|^2 + |r^s|^2$ , and using  $\kappa = t^p/t^s$  and  $\kappa = r^p/r^s$  for transmitted and reflected waves, respectively, the Faraday rotation  $\beta$  and ellipticity  $\eta$  angles are determined by

$$\beta = \frac{1}{2} \arctg \frac{2Re(\kappa)}{1 - |\kappa|^2}, \quad \eta = \frac{1}{2} \arcsin \frac{2Im(\kappa)}{1 + |\kappa|^2}, \tag{13}$$

which schematically are represented in Fig. 1b. Generally, even with a linearly polarized incident wave, the transmitted and reflected waves are elliptically polarized.

### II. Kolakoski sequences generation rule

A Kolakoski self-generating sequence (KSGS) is defined by the property that it equals the sequence of its run lengths, where a run is a maximal subsequence of consecutive identical letters [37–41]. An infinite one-sided Kolakoski sequence

$$\zeta = \underbrace{22}_2 \underbrace{11}_2 \underbrace{2}_1 \underbrace{1}_1 \underbrace{22}_2 \underbrace{1}_1 \underbrace{22}_2 \dots \tag{14}$$

which started from digit “2” is called the K(2, 1) sequence. In addition the sequence

$$\zeta' = 1\zeta = 122112122122\dots \tag{15}$$

is the other type of the Kolakoski sequence which started from digit “1” and is called K(1, 2).

Classical and generalized Kolakoski sequences can be generated by an algorithm that is similar to those of Fibonacci or Thue-Morse sequences. The rules for the generation scheme of the classical Kolakoski self-generating sequence are briefly: (1) the classical sequence is formed from a pair of one-digit numbers 1 and 2; (2) The sequence consists of blocks of single and double 1 s and 2 s, each block is containing a different digit or a pair of digits compared to the previous block; (3) the  $j$ -th block of the sequence has length  $l_j = a_j$  (where  $a_j$  is the  $j$ -th element of the sequence); (4) In the sequence, there cannot be more than two neighbors with the same number; (5) every time when we “read” a new number, we alternate between writing 1 and 2. For example, the K(2, 1) sequence can be obtained from Eq. by starting with initiator 2 and iterating two alternating substitutions [37]. The number of generation stages of the Kolakoski sequence is defined as  $\sigma$  and the total number of layers in the structure is  $\mathcal{N}$ .

### 3 Numerical calculation and discussion

For the realization of the main features of the magneto-optical response of Kolakoski-based MPCs, we assume that magnetic M and nonmagnetic N layers are corresponded to digits “1” and “2” in the K(1, 2) sequence, respectively. For numerical calculations, as Ref [42], we consider the magnetic layers M to be Ce doped yttrium iron garnet Ce:YIG, with  $n_{YIG}=2.21$  and  $\epsilon_{xy}=0.009i$  at  $\lambda=1.55\mu\text{m}$  and, nonmagnetic layers N gadolinium gallium garnet GGG with  $n_{GGG}=1.926$ . We suppose that MPC is surrounded by the medium with refractive index, averaged over MPC, in order to avoid the effect related to Fresnel reflections at the surface of MPC [32], *i.e.*  $n=2.0$ . The layer thicknesses are chosen to be  $d_M = \lambda/4n_{YIG}$  and  $d_N = \lambda/4n_{GGG}$ .

The transmission, Faraday, and ellipticity rotation spectra of Kolakoski-based MPCs are presented in Fig. 2. In order to study the effect of the number of layers on magneto-optical responses, we considered MPCs with the number of layers,  $\mathcal{N}=60$  and  $\mathcal{N}=85$ . Here  $\omega D/2\pi c$  is the dimensionless frequency and  $D = d_M + d_N$ . It is important to note that the transmission spectra of both of MPCs demonstrate symmetrical profiles around certain normalized frequencies,

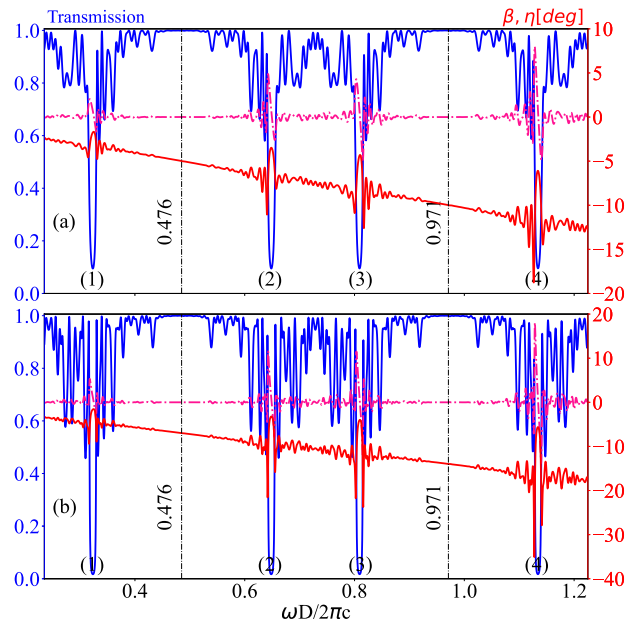


**Fig. 2** The response to the normal incident linearly polarized light: The transmission coefficient  $T$  (blue solid line), Faraday  $\beta$  (red solid line), and ellipticity  $\eta$  (pink dashed-dotted line) vs the normalized frequency for **a**  $\mathcal{N}=60$  and **b**  $\mathcal{N}=85$

e.g.  $\omega D/2\pi c = 0.729$ . Moreover, they show bands with high and low levels of transmission, which are referred to as pseudo-stopbands and pseudo-passbands. The interference

of the reflected waves from the different boundaries and field localization inside the structures cause oscillations in pseudo-passbands and appearing sharp transmission peaks (localized modes) within the pseudo-stopbands, respectively [29]. The total number of layers in the MPC determines the number of resonances, their spectrum, width, location, and magnitude. Figure 2 illustrates that the boundaries of the bands become sharper with an increase in  $\mathcal{N}$  and that more and more resonant transmission peaks emerge in the center of the pseudo-stopbands. The peaks get narrower and their magnitudes approach 1, Due to the lack of dispersion and loss in the materials. Also, some additional pseudo-stopbands appear in the spectra, which the number of them can be controlled with the parameter  $\mathcal{N}$ . Besides, Faraday and ellipticity rotation increase with increasing  $\mathcal{N}$  and frequency of incident light.

The exact values of transmission, Faraday, and ellipticity rotations for pseudo-stopbands (1–4) in Fig. 2 are provided in Fig. 3. The displayed values are calculated in transmission peaks. Furthermore, for  $\mathcal{N}=60$ , the structure achieves a flat-top edge-mode with bandwidth of approximately 5THz, as shown with double-ended green arrows in Fig. 3a–d. The flat transmittance of polarized linear waves and the increased Faraday rotation confirm the feasibility of using tunable magneto-optic filters for transmission. Reduction of the bandgaps width and increase of Faraday rotation with increasing number of layers is also evident. Besides, for the additional information about the 1D aperiodic MPCs, we

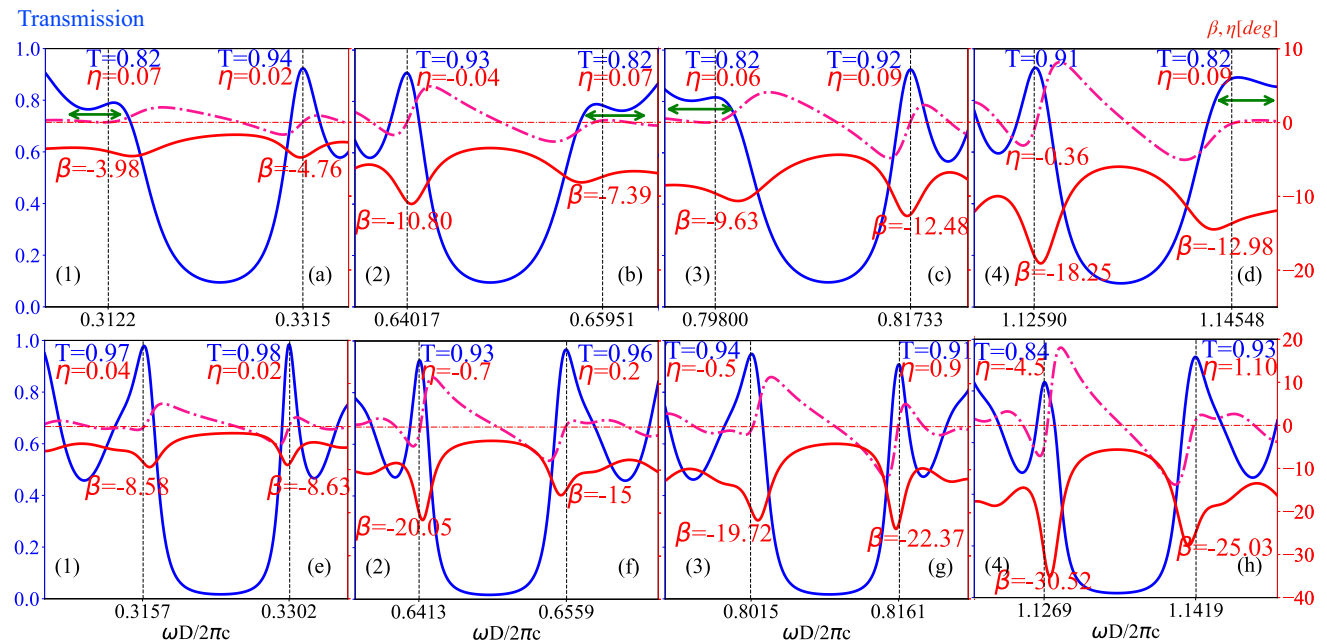


**Fig. 3** **a** The response to the normal incident linearly polarized light: The transmission coefficient  $T$  (blue-solid line), Faraday  $\beta$  (red solid line), and  $\eta$  ellipticity (pink dashed-dotted line) vs the normalized fre-

quency. **a–d** for  $\mathcal{N}=60$  and **e–h** for  $\mathcal{N}=85$ . Vertical lines indicate the location of transmission peaks

have calculated the features of the reflected wave, as seen in Fig. 4. Areas with constant Faraday rotation and zero ellipticity are highlighted in the middle of the pseudo-stopbands. There is not much change in Faraday rotation of the reflected wave as the number of layers and the frequency of incident light increase. In this study, dispersion and loss in layers were ignored, resulting in  $R+T=1$ , however considering them can modify magneto-optical responses and provide interesting results [43, 44].

It is worth noting that as shown in [21], intrinsic symmetry of self-similarity of Kolakoski-based MPCs manifests itself in the structure of its Fourier spectra and the structural correspondence of the Fourier and the transmission spectra is significant. This indicates the Fourier transformation of this aperiodic MPC reveals important information about the transmission and reflection spectra, e.g. the position of pseudo-bandgaps and pseudo-stopbands in the spectra, which can be addressed in the next studies.

Comparing the magneto-optical responses of Kolakoski-based MPCs with different arrangements of defective, aperiodic, and quasiperiodic can yield very interesting results. Here, since for numerical calculations, we used the parameters provided in the Ref. [42], we compare responses of the Kolakoski and two-defects MPCs with the same number of layers,  $\mathcal{N}=125$ . As shown in Fig. 5a, the transmission of the second defect mode in the defective MPC decreased significantly, which makes it practically useless. However, in the Kolakoski-based MPC similar to previous cases in Fig. 2, not only edge modes' transmittance at higher frequencies

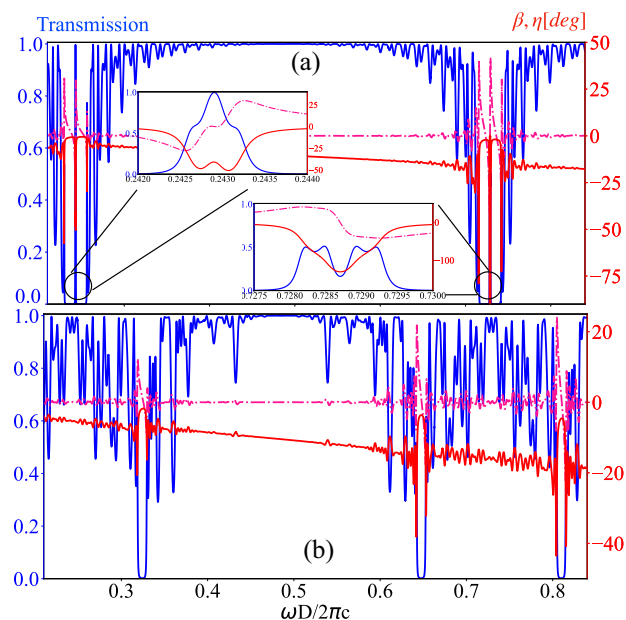


**Fig. 5** The response to the normal incident linearly polarized light: The transmission coefficient  $T$  (blue solid line), Faraday  $\beta$  (red solid line), and ellipticity  $\eta$  (pink dashed-dotted line) vs the normalized frequency for **a** two-defect [42] and **b** Kolakoski-based MPC with  $\mathcal{N}=125$

has not decreased, but the Faraday rotation of these modes has increased, which makes them an excellent candidate for fabricating multicolor filters.

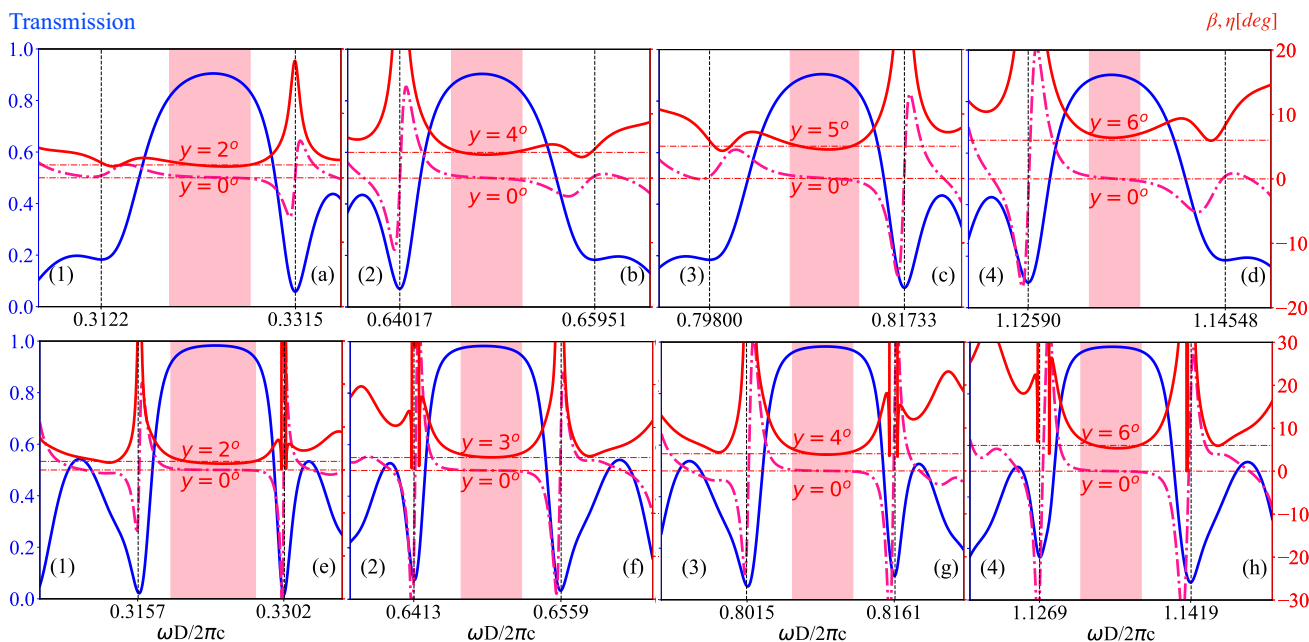


**Fig. 4** **a** The response to the normal incident linearly polarized light: The reflection coefficient  $R$  (blue-solid line), Faraday  $\beta$  (red-solid line), and  $\eta$  ellipticity (red dashed-dotted line) vs the normalized frequency for **a-d**  $\mathcal{N}=60$ , and **e-h**  $\mathcal{N}=85$

In order to better understand the physical mechanisms for the transmission properties and enhancement of the Faraday rotation, we calculate the distribution of intensities of the electric field  $|E|^2$  in aperiodic MPCs with  $N=60$  and  $N=85$  at the frequency of the tunneling modes  $\omega D/(2\pi c) = 0.798$  and  $\omega D/(2\pi c) = 0.801$ , respectively. As shown in Fig. 6, strongly localized electric fields of the tunneling modes are formed inside the structures. This enhancement originates basically from the fact that the strong scattering of light waves due to the high inhomogeneity of the Kolakoski multilayer leads to the formation of resonant cavities. Therefore, the local field will be intensively enhanced and localized in the magnetic optical layers, which can realize high transmission and a large Faraday rotation angle of the designed frequency simultaneously.

At last, since new magneto-optical properties appear when light is incident on the MPCs at an oblique angle, we study the influence of incident angle  $\theta$  on the magneto-optical response of designed aperiodic MPCs. The dependence of

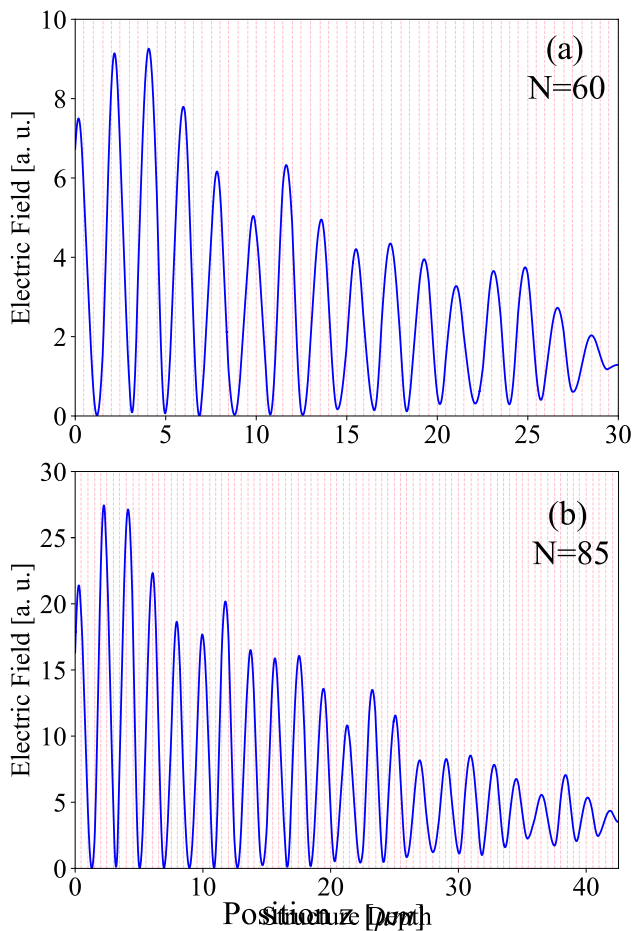


**Fig. 6** Distribution of electric field intensity in the aperiodic MPCs with **a**  $N=60$  and **b**  $N=85$  at the normalized frequency  $\omega D/(2\pi c) = 0.798$  and  $\omega D/(2\pi c) = 0.801$ , respectively. The dashed lines show the border between different layers

the transmission and Faraday rotation on the incident angle and normalized frequency for different polarization of incident light is shown in Fig. 7. By taking advantage of the oblique geometry, polarization degeneracy between TE and TM which exists at normal incidence is removed. Besides, as the incident angle increases, all the resonant features as edges of the bandgaps and resonant peaks experience a significant “blue” shift. This blue shift shows the possibility of using Kolakoski-based MPCs as tunable magneto-optical devices such as filters, polarizers, and shutters. For TM polarization, the bandgaps (1–4) in Fig. 2 become slightly wider when the angle increases, but are drastically reduced to zero for TE polarization. Practically speaking, this effect is significant.

## 4 Conclusion

In conclusion, in this paper, we have studied the magneto-optical properties of the novel type of one-dimensional aperiodic multilayered structures formed according to the generalized Kolakoski sequence generation rules. On the basis of the  $4 \times 4$ -block-representation transfer matrix formulation, the expressions for calculating the reflection and transmission coefficients and related Faraday and ellipticity angles are obtained. The results reveal that high transmittance and large Faraday rotation angle can be simultaneously realized in the aperiodic 1D-MPCs based on Kolakoski sequences. We have shown that the magneto-optical properties are sensitive to a change in incident angle, polarization,

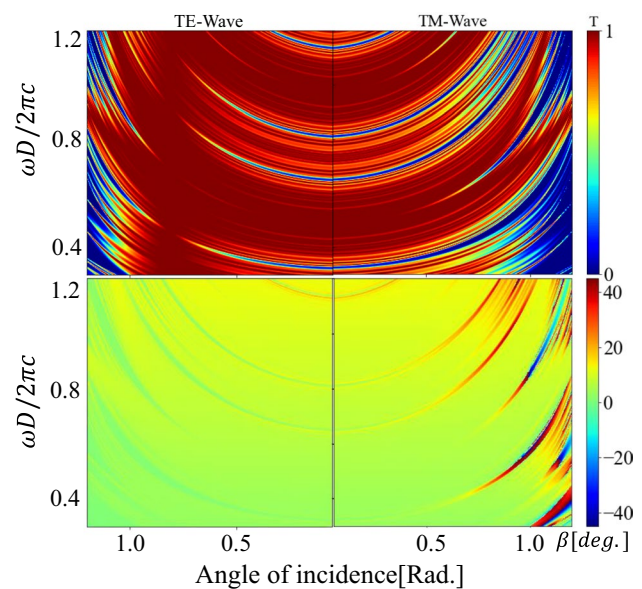


**Fig. 7** Two-dimensional plots of Faraday rotation and transmissivity evolution with the incidence angle  $\theta$  and normalized frequency for TE and TM incidence wave in aperiodic MPC with  $N=60$

and frequency of light as well as the number of layers. Consequently, tunability of frequency range and the width of the bandgaps of transmission and reflection spectra, as well as high Faraday rotation, have exposed these devices as effective candidate for designing spectral- and polarization-selective optical components and Faraday rotators.

**Funding** OpenAccess funding enabled and organized by Projekt DEAL.

**Data availability** The data that support the findings of this study are available from the corresponding authors upon reasonable request.

**Open Access** This article is licensed under a Creative Commons Attribution 4.0 International License, which permits use, sharing, adaptation, distribution and reproduction in any medium or format, as long as you give appropriate credit to the original author(s) and the source, provide a link to the Creative Commons licence, and indicate if changes were made. The images or other third party material in this article are included in the article's Creative Commons licence, unless indicated otherwise in a credit line to the material. If material is not included in the article's Creative Commons licence and your intended use is not permitted by statutory regulation or exceeds the permitted use, you will need to obtain permission directly from the copyright holder. To view a copy of this licence, visit <http://creativecommons.org/licenses/by/4.0/>.

## References

1. T. Parvini, M. Tehranchi, S. Hamidi, *Photonics Nanostructures: Fundam. Appl.* **25**, 25 (2017)
2. S. Hamidi, T. Parvini, M. Tehranchi, *Appl. Phys. A* **111**, 525 (2013)
3. F.A. Zarif, M.K. Nezhad, H.R.M. Rezaeiun, *Photonics Nanostructures: Fundam. Appl.* **36**, 100726 (2019)
4. M. Khani, M. Khazaei Nezhad, H. Rastegar Moghaddam Rezaeiun, *Eur. Phys. J. Plus* **133**, 1 (2018)
5. T. Parvini, M. Tehranchi, S. Hamidi, *Appl. Phys. A* **118**, 1447 (2015)
6. F.-F. Stiewe, T. Winkel, Y. Sasaki, T. Tubandt, T. Kleinke, C. Denker, U. Martens, N. Meyer, T.S. Parvini, S. Mizukami et al., *Appl. Phys. Lett.* **120**, 032406 (2022)
7. D. Yang, J. Liang, C. Zhou, L. Sun, R. Zheng, S. Luo, Y. Wu, J. Qi, *Adv. Opt. Mater* **4**, 1944 (2016)
8. M. Seifouri, V. Fallahi, S. Olyae, *Photonic Netw. Commun.* **35**, 225 (2018)
9. Y.-H. Liu, L. He, L.-J. Dong, L.-X. Liu, Y.-L. Shi, C.-Q. Yang, *J. Appl. Phys* **114**, 063105 (2013)
10. A.M. Grishin, S. Khartsev, H. Kawasaki, *Appl. Phys. Lett.* **90**, 191113 (2007)
11. Y. Trabelsi, N.B. Ali, M. Kanzari, *Microelectron. Eng.* **213**, 41 (2019)
12. S. Khartsev, A.M. Grishin, *Appl. Phys. Lett.* **87**, 122504 (2005)
13. A.B. Khanikaev, M. Steel, *Opt. Express* **17**, 5265 (2009)
14. C. He, X.-C. Sun, Z. Zhang, C.-S. Yuan, M.-H. Lu, Y.-F. Chen, C. Sun, *Opt. Express* **21**, 28933 (2013)
15. Z. Guo, F. Wu, C. Xue, H. Jiang, Y. Sun, Y. Li, H. Chen, *J. Appl. Phys* **124**, 103104 (2018)
16. H. Da, C. Xu, Z. Li, *Phys. Lett.A* **345**, 459 (2005)
17. Y.S. Dadoenkova, N.N. Dadoenkova, I.L. Lyubchanskii, J.W. Klos, M. Krawczyk, *IEEE Trans. Magn.* **53**, 1 (2017)
18. M. Bellingeri, A. Chiasera, I. Kriegel, F. Scotognella, *Opt. Mater.* **72**, 403 (2017)
19. K.Y. Bliokh, S.A. Gredeskul, P. Rajan, I.V. Shadrivov, Y.S. Kivshar, *Phys. Rev. B* **85**, 014205 (2012)
20. R. Abdi-Ghaleh, A. Namdar, *Physica B: Condens. Matter* **501**, 57 (2016)
21. A. Averchenko, N.Y. Konopaltseva, P. Korolenko, A.Y. Mishin, *Bull. Russ. Acad. Sci.: Phys.* **82**, 1383 (2018)
22. L. Dal Negro, N.-N. Feng, A. Gopinath, *J. Opt. A: Pure Appl. Opt.* **10**, 064013 (2008)
23. R. da Silva, F. Zanetti, M. Lyra, I. de Oliveira, *Mol. Cryst. Liq. Cryst.* **657**, 11 (2017)
24. F. Ghorbani-Oranj, R. Abdi-Ghaleh, B. Roumi, K. Jamshidi-Ghaleh, A. Madani, Y. Zhou, *Phys. B: Condens. Matter* **636**, 413835 (2022)
25. W. Hsueh, S. Wun, Z. Lin, Y. Cheng, *J. Opt. Soc. Am. B* **28**, 2584 (2011)
26. H. Azarshab, A. Gharaati, *Microelectron. Eng.* **198**, 93 (2018)
27. L. Kroon, E. Lennholm, R. Riklund, *Phys. Rev. B* **66**, 094204 (2002)
28. T. Parvini, M. Tehranchi, S. Hamidi, S. Sarkarati, *J. Appl. Phys.* **118**, 183108 (2015)
29. V.R. Tuz, V.I. Fesenko, I.A. Sukhoivanov, in *Integrated optics: physics and simulations*, Vol. 8781 (International Society for Optics and Photonics, 2013) p. 87811C
30. V.I. Fesenko, V.R. Tuz, O.V. Shulika, I.A. Sukhoivanov, *Nanophotonics* **5**, 556 (2016)
31. H. Kato, T. Matsushita, A. Takayama, M. Egawa, K. Nishimura, M. Inoue, *J. Appl. Phys* **93**, 3906 (2003)
32. J. Geddes III, *Frontiers in optical technology: Materials and devices*, (2006)
33. A.K. Zvezdin, V.A. Kotov, *Modern magneto-optics and magneto-optical materials* (CRC Press, 1997)
34. J.W.K. Los, I.L. Lyubchanskii, M. Krawczyk, P. Gruszecki, S. Mieszczyk, J. Rychly, Y.S. Dadoenkova, N.N. Dadoenkova, in *Optomagnonic Structures: Novel Architectures for Simultaneous Control of Light and Spin Waves* (World Scientific, Singapore, 2021), pp.79–134
35. L. Brekhovskikh, *Waves in layered media*, vol. 16 (Elsevier, 2012)
36. E. Shapovalov, Y. Lee, *Frontiers in Optical Technology: Materials and Devices*, **23**, (2007)
37. B. Sing, *J. Non-Cryst. Solids* **334**, 100 (2004)
38. K. Lambropoulos, C. Simserides, *Phys. Rev. E* **99**, 032415 (2019)
39. V.I. Fesenko, *Prog. Electromagn. Res. M* **41**, 33 (2015)
40. V. Fesenko, *Waves Random Complex Media* **24**, 174 (2014)
41. V.I. Fesenko, V.R. Tuz, I.A. Sukhoivanov, in *Terahertz and Mid Infrared Radiation: Detection of Explosives and CBRN (Using Terahertz)* (Springer, Netherlands, 2014), pp.25–32
42. I. Lyubchanskii, N. Dadoenkova, M. Lyubchanskii, E. Shapovalov, A. Zabolotin, Y. Lee, T. Rasing, *J. Appl. Phys.* **100**, 096 (2006)
43. M. Golshani, S. Weimann, K. Jafari, M.K. Nezhad, A. Langari, A. Bahrampour, T. Eichelkraut, S. Mahdavi, A. Szameit, *Phys. Rev. Lett.* **113**, 123903 (2014)
44. M.K. Nezhad, M. Golshani, D. Mirshamsi, *Opt. Commun.* **405**, 387 (2017)

**Publisher's Note** Springer Nature remains neutral with regard to jurisdictional claims in published maps and institutional affiliations.